Predictive modeling of morbidity and mortality in COVID-19 hospitalized patients and its clinical implications.

Joshua M. Wang, Wenke Liu, Xiaoshan Chen, Michael P. McRae, John T. McDevitt, David Fenyo

Table of Contents

Predictive modeling of morbidity and mortality in COVID-19 hospitalized patients and its clinical implications.

Joshua M. Wang[1] BSc; Wenke Liu[1] PhD; Xiaoshan Chen[1] BSc; Michael P. McRae[2] PhD; John T. McDevitt[2] PhD; David Fenyo[1] PhD

[1]NYU Grossman School of Medicine New York US
[2]New York University College of Dentistry New York US

Corresponding Author:
David Fenyo PhD
NYU Grossman School of Medicine
435 E 30th St
9th Floor, Room 907
New York
US

Abstract

Background: Retrospective study of COVID-19 positive patients treated at NYU Langone Health (NYULH).

Objective: Identify clinical markers predictive of disease severity to assist in clinical decision triage and provide additional biological insights into disease progression.

Methods: Clinical activity of 3740 de-identified patients at NYULH between January and August 2020. Models were trained on clinical data during different parts of their hospital stay to predict three clinical outcomes: deceased, ventilated, or admitted to ICU.

Results: XGBoost model trained on clinical data from the final 24 hours excelled at predicting mortality (AUC=0.92, specificity=86% and sensitivity=85%). Respiration rate was the most important feature, followed by SpO2 and age 75+. Performance of this model to predict the deceased outcome extended 5 days prior with AUC=0.81, specificity=70%, sensitivity=75%. When only using clinical data from the first 24 hours, AUCs of 0.79, 0.80, and 0.77 were obtained for deceased, ventilated, or ICU admitted, respectively. Although respiration rate and SpO2 levels offered the highest feature importance, other canonical markers including diabetic history, age and temperature offered minimal gain. When lab values were incorporated, prediction of mortality benefited the most from blood urea nitrogen (BUN) and lactate dehydrogenase (LDH). Features predictive of morbidity included LDH, calcium, glucose, and C-reactive protein (CRP).

Conclusions: Together this work summarizes efforts to systematically examine the importance of a wide range of features across different endpoint outcomes and at different hospitalization time points.

Preprint Settings

1) Would you like to publish your submitted manuscript as preprint?
    Please make my preprint PDF available to anyone at any time (recommended).
    Please make my preprint PDF available only to logged-in users; I understand that my title and abstract will remain visible to all users.
    Only make the preprint title and abstract visible.
✔ **No, I do not wish to publish my submitted manuscript as a preprint.**
2) If accepted for publication in a JMIR journal, would you like the PDF to be visible to the public?
✔ **Yes, please make my accepted manuscript PDF available to anyone at any time (Recommended).**
    Yes, but please make my accepted manuscript PDF available only to logged-in users; I understand that the title and abstract will remain v
    Yes, but only make the title and abstract visible (see Important note, above). I understand that if I later pay to participate in <a href="http

Original Manuscript

Title: Predictive modeling of morbidity and mortality in COVID-19 hospitalized patients and its clinical implications.

Authors: Joshua M. Wang[1], Wenke Liu[1], Xiaoshan Chen[2], Michael P. McRae[3], John T. McDevitt[3], David Fenyö[1*]

1. Institute for Systems Genetics; Department of Biochemistry and Molecular Pharmacology, NYU Grossman School of Medicine, New York, NY, 10016, USA
2. Department of Medicine, NYU Grossman School of Medicine, New York, NY, 10016, USA
3. Department of Biomaterials, Bioengineering Institute, New York University College of Dentistry, New York, NY, United States

*Corresponding author; email: David.Fenyo@nyulangone.org

ABSTRACT

Objective: Retrospective study of COVID-19 positive patients treated at NYU Langone Health (NYULH) to identify clinical markers predictive of disease severity to assist in clinical decision triage and provide additional biological insights into disease progression.

Methods: Clinical activity of 3740 de-identified patients at NYULH between January and August 2020. Models were trained on clinical data during different parts of their hospital stay to predict three clinical outcomes: deceased, ventilated, or admitted to ICU.

Results: XGBoost model trained on clinical data from the final 24 hours excelled at predicting mortality (AUC=0.92, specificity=86% and sensitivity=85%). Respiration rate was the most important feature, followed by SpO2 and age 75+. Performance of this model to predict the deceased outcome extended 5 days prior with AUC=0.81, specificity=70%, sensitivity=75%. When only using clinical data from the first 24 hours, AUCs of 0.79, 0.80, and 0.77 were obtained for deceased, ventilated, or ICU admitted, respectively. Although respiration rate and SpO2 levels offered the highest feature importance, other canonical markers including diabetic history, age and temperature offered minimal gain. When lab values were incorporated, prediction of mortality benefited the most from blood urea nitrogen (BUN) and lactate dehydrogenase (LDH). Features predictive of morbidity included LDH, calcium, glucose, and C-reactive protein (CRP).

Conclusion: Together this work summarizes efforts to systematically examine the importance of a wide range of features across different endpoint outcomes and at different hospitalization time points.

INTRODUCTION

The first cluster of SARS-CoV-2 was reported in Wuhan, Hubei Province on December 31, 2019. Inciting symptoms remarkably similar to pneumonia, the disease quickly traveled around the world, earning its pandemic status by the World Health Organization on March 11, 2020. Although the first wave has since passed for hardest-hit regions such as New York City (NYC) and most of Asia, a resurgence of cases has already been reported in Europe and record new cases tallied in the Midwest and rural United States (US). As of November 12th, the US alone logged its highest tally to date with a 317% growth over the preceding 30 days [1]. The coronavirus disease (COVID-19) is far from seeing the end of its days and there remains a compelling need to prioritize care and resources for patients at elevated risk of morbidity and mortality.

Previous work building machine learning models used patient data from Tongji Hospital [2,3] (Wuhan, China), Zhongnan Hospital [4] (Wuhan China), Mount Sinai Hospital [5] (NYC, US), and NYU Family Health Center [6] (NYC, US). Surprisingly, clinical features selected varied widely across studies. For example, while McRae et al.'s 2-tiered model [6] trained on 701 NYC patients to predict mortality was based on actual age, C-reactive protein (CRP), procalcitonin, and D-dimer, Yan et al.'s model [2] trained on 485 patients from Wuhan selected lactate dehydrogenase (LDH), lymphocyte count, and CRP as the most predictive for mortality. Variations in selected features differed greatly even when trained to predict similar outcomes on data from patients of the same city. Yao et al.'s model [3] was trained on 137 patients from Wuhan and relied on 28 biomarkers in their final model to predict morbidity. Given the differences among prior models, some of which were driven by domain-specific knowledge, we decided to systematically examine the importance of a wide range of features across different endpoint outcomes and at different hospitalization time points.

This study analyzes retrospective PCR-confirmed COVID-19 inpatient data collected at NYU Langone Hospital spanning 1/1/2020 to 8/7/2020 to predict three sets of clinical outcomes: alive vs deceased, ventilated vs not ventilated, or ICU admitted vs not ICU admitted. The clinical information of 3,740 patient encounters included demographic data (age, sex, insurance, past diagnosis of diabetes, presence of cardiovascular comorbidities), vital signs (SpO2, pulse, respiration rate, temperature, systolic blood pressure, diastolic blood pressure), and the 50 most frequently ordered lab tests in our dataset. Models were developed using two methods: logistic regression with feature selection using Least Absolute Shrinkage and Selection Operator [7] (LASSO) and gradient tree boosting with XGBoost [8]. An explainable algorithm, such as logistic regression, provides easy to interpret insights into the features of importance. Conversely, the larger model capacity of XGBoost better handles data complexities to explore the extent that predictive performance can be optimized. Together, this study aims to provide a holistic survey of the clinical underpinnings of disease etiology for COVID-19 patients admitted to NYU Langone Hospital. In addition, we seek to explore the prospects of building models that are sufficiently competent to be effective decision support tools.

METHODS

Ethics Statement

Ethics exemption/waiver was confirmed through the Institutional Review Board at NYU Grossman School of Medicine. An IRB self-certification form was completed to ensure that the subsequent research did not fall under human subject research, and so no IRB approval is required. The COVID-19 De-identified Clinical Database was stripped of all unique identifiers prior to receiving data. In addition, all dates were shifted by an arbitrary number of days for each patient. These safeguards ensure that patient data cannot be re-identified, and thus are not subject to HIPAA restrictions on research use, and do not require IRB approval.

Data Collection

Clinical activity of patients at NYULH was obtained from Epic between 1/1/2020 and 8/7/2020. The data was stripped of all unique identifiers (MRN, names, etc.) and actual dates were shifted by an arbitrary number of days for each patient, which ensures that no data is subject to HIPAA restrictions and thus does not require IRB approval.

Clinical Data Pre-processing and Cleaning

Our dataset contained 206,677 patients who were tested for COVID-19, of which 12,473 tested positive (Supplemental Figure 1). Not all patients who tested positive sought hospital care, and without vital signs or lab values, these patients were excluded from analysis. In addition, a majority of the 175,507 patients diagnosed with COVID-19 did not receive in-house PCR tests, which makes it difficult to distinguish which hospital encounters were related to seeking COVID-19 treatment. Thus, only patients for which we could confirm a positive PCR test as reported by NYULH were included. The timestamp of the first encounter in which a PCR test returned positive was used as the starting date for each patient, and the ending date as either the time of discharge for that encounter or time of death. The clinical features that were collected for each patient along with their definitions and additional processing steps are described as follows:

Categorical features

- Binned ages:
  To comply with HIPAA restrictions on research use, exact patient ages were removed and binned into predefined ranges, as determined by the Data Handling Committee.
    - 0-17
    - 18-44
    - 45-64
    - 65-74
    - 75+
- Gender:
    - 0 for Female
    - 1 for Male
- Insurance type:
    - 0 for PPO
    - 1 for EPO, HMO, POS, Indemnity, Medicare, Medicare Managed Care, No Fault, Workers' Compensation
    - 2 for Medicaid, Medicaid Managed Care
- Diabetes:
    - 1 for any past diagnosis mentioning diabetes
    - 0 otherwise

- Cardiovascular Comorbidities:
    - 1 for any of the following ICD-10 diagnosis codes: I10-I16 (hypertensive diseases), I20-I25 (ischemic heart diseases), I50 (heart failure), I60-I69 (cerebrovascular diseases), and I72 (other aneurysms)
    - 0 otherwise

Continuous Features

For each of the following continuous features, multiple periodic measurements were recorded for each patient by vital signs monitors. Measurements were binned into 24 hour windows that began from time of hospitalization. Within each window, values were averaged. Values were then standardized to a mean of zero and variance of one. For each day, encounters without all features listed below were removed and not imputed.

- SpO2 (%)
- Pulse (bpm)
- Respiration Rate (bpm)
- Temperature (°F)
- Systolic Blood Pressure (mmHg)
- Diastolic Blood Pressure (mmHg)

Outcomes

- Living status:
    - 0 for Alive
    - 1 for Dead
- Ventilation at any point during hospitalization:
    - 0 for No (did not receive any form of ventilation or only received non-invasive treatments (ex. nasal cannula, non-rebreather mask etc.)
    - 1 for Yes (received mechanical ventilation treatment)
- ICU admission for any duration during hospitalization:
  Criteria determined by medical triage team, balanced between disease severity and hospital resource availability.
    - 0 for No
    - 1 for Yes

Lab Data Selection and Cleaning

Lab tests with at least 50% completeness during the first 24 hours for all encounters were considered. Of the 54 lab tests meeting these requirements, EGFR (non-African and African American) was removed due to the formula's dependency on lab features already selected (creatinine). In addition, the placeholder for ordering a CBC with Differential test and COVID PCR tests were also removed. Missing lab values were imputed using the multivariate imputation by chained equations (MICE) algorithm. Five imputations were generated using predictive mean matching. After imputation, lab values were shifted up by one and log transformed. Model-building approaches that incorporated lab features had individual models built for each imputation.

Feature Selection and Model Building

All models were trained with a train:validation split of 90:10. Features for logistic regression were selected using Least Absolute Shrinkage and Selection Operator (LASSO) and optimized for a penalty parameter that was one standard error above the minimum deviance for additional shrinkage. The XGBoost parameters were identified using a hyper-parameter search within the following constraints: nrounds: 1000, eta: 0.3, 0.1, 0.01, max_depth = 2, 3, 4, 5, 6, 7, 8, min_child_weight = 0 to 1 by 0.1 increments and gamma = 0 to 1 by 0.1 increments. To account for class imbalance,

sample-weighted loss was employed when calculating the loss.

For models that were trained on the final day of discharge/death, the performance on predicting outcomes in all preceding days was evaluated on the entire dataset rather than just a 10% subset. Data from previous days was not used in the training of these endpoint models, and thus can all serve as validation.

Time Series Modeling

In each feature setting, all variables were combined and missing values at each time point were imputed with the immediate previous value (forward filling). After imputation, time points with incomplete feature measurements were discarded, and each patient record was segmented into non-overlapping sequences of length 8. Patients were randomly assigned to training, validation and testing groups in an 8:1:1 ratio for three independent splits. All models were implemented in Python with built-in units in TensorFlow 2 and Keras [9]. Logistic regression was fit as a neural network with the sigmoid output node immediately after the input layer. For MLP, RNN, GRU and LSTM models, a hidden layer of size 8 was added, and the time series models (RNN, GRU and LSTM) were unrolled over 8 time points and trained with true labels provided at each step. Five randomly initialized models were trained for all architectures on each training/validation/testing split. Model performance was evaluated based on all single time point predictions and reported as mean value across all splits.

RESULTS

More than half of all patients in our dataset were over the age of 65, with pediatric patients (0-17) having the lowest representation (Fig. 1A, Supplemental Table S1). Generally, the proportion of deceased patients increased with age, peaking at 38% for 75+, 16% for 45-64, and 0% for pediatric patients. Most patients who were either ventilated or admitted to the ICU belonged to the 65-74 age group followed by 45-64 and 75+.

Aggregation of values for commonly acquired clinical metrics over normalized time courses offered meaningful insights into disease progression. Each patient's hospitalization stay was segmented into 5% windows and clinical metrics were averaged within each bin (Fig. 1B). We first examined the difference of average vital sign measurements between cohorts with different outcomes. The value of SpO2 was statistically different for all three outcome comparisons in the first 5% of hospitalization time (Wilcoxon test; $P<.001$, $P<.001$, $P<.001$). Over the clinical time course, the difference in SpO2 averages increased the most for those that deceased, followed by ICU admitted and ventilated. Differences in respiration rate followed a similar adverse trend with breaths/min increasing the most for those that deceased, followed by ventilated and ICU admitted. The divergence was present even after accounting for overlapping deceased patients. When subsetted for only those that survived, ventilated patients had 2.91 more breaths/min (Wilcoxon test; $P<.001$), and ICU admitted patients had 2.90 more breaths/min (Wilcoxon test; $P<.001$). At beginning of time course, differences in temperature were small (0.05°F, 0.11°F, and 0.06°F respectively), and not statistically significant for those deceased (Wilcoxon test; $P=0.13$), but was for those ventilated (Wilcoxon test; $P<.001$) or admitted to ICU (Wilcoxon test; $P<.001$). Pulse differences at beginning were not significantly different for those ventilated (Wilcoxon test; $P=0.29$), but was for those deceased (Wilcoxon test; $P<.001$) and ICU admitted (Wilcoxon test; $P<.001$). Systolic and diastolic blood pressures were continuously lower for patients with worse outcomes in this dataset.

To assess the effectiveness of these vital signs to triage clinical outcomes, only data collected in the first 24 hours after admission was initially considered. Specifically for the ventilation outcome, respiration rates and SpO2 levels may be influenced by when mechanical ventilation was administered. Of 3740 encounters, 7% were ventilated within the first 24 hours of admission. To assess the bias that early administration of mechanical ventilation during the first 24 hours may have on respiration rate and SpO2 levels, the distribution of values was compared against a filtered subset containing only values recorded prior to start of ventilation. At the per-encounter level, the difference in respiration rates (Wilcoxon test; $P=0.26$, Supplemental Fig. 2A) and SpO2 levels (Wilcoxon test; $P=0.20$, Supplemental Fig. 2B) were not significantly different. Given that 1) 93% of encounters were not influenced by early ventilation treatment, 2) the insignificant difference in distributions, and 3) the desire to keep feature selection consistent across models, all values recorded within the first 24 hours were included. For each encounter, continuous features with multiple recordings (SpO2, pulse, respiration rate, temperature, systolic blood pressure, diastolic blood pressure) were averaged, and then standardized to mean of 0 and standard deviation of 1.

For logistic regression, features were selected using LASSO with 10-fold cross validation. Grid search was used to optimize XGBoost parameters (Supplemental Table S2). When trained on data from the first 24 hours, the logistic model had AUC performances of 0.79, 0.80, 0.77, specificities of 59%, 78%, 79%, and sensitivities of 86%, 74%, 68% respectively (Fig. 2A). XGBoost performed similarly with AUC performances of 0.80, 0.80, 0.77, specificities of 59%, 83%, 69%, and sensitivities of 86%, 70%, 77% respectively (Fig. 2B).

In both logistic regression and gradient tree boosting settings, features of importance varied across clinical outcomes (Fig. 2C). For logistic regression models of the three outcomes, respiration rate, SpO2 and cardiovascular comorbidity were among predictive features, but age groups were selected only for predicting mortality. For boosting tree models, feature importance measures showed that respiration rate was consistently the most important feature for all three outcomes, and age_18-44 was the second most important feature only for vital status. Respiration rate and SpO2 were important for predicting all three outcomes. Differences in temperature were not strongly predictive in any cohort in either model, and its insignificant difference in the deceased outcome group together suggests that its role in screening for increased disease severity may not be dependable.

The 50 most frequently collected labs and their relative importance were also studied. A t-SNE plot (Fig. 3A) suggests lack of clustering among lab features, and overall low correlation (Fig. 3B) in pairwise comparisons ($|\mu|$ = 0.08, $|\sigma|$ = 0.10). Local pockets of correlation ($|cor|>=0.83$) were identified between (hemoglobin, hematocrit, red blood cell count), (absolute neutrophils, white blood cell count), and (bilirubin direct, bilirubin total). Each of these sets measures variables that are clinically interdependent and thus expected.

Incorporating lab features into the predictive models marginally improved performance. Logistic regression had AUC performances of 0.83, 0.81, 0.78, specificities of 68%, 70%, 69%, and sensitivities of 85%, 83%, 74% respectively (Fig. 4A). The XGBoost model performed better with AUC increasing to 0.84, 0.79, 0.78, specificities of 71%, 72%, 65%, and sensitivities of 83%, 73%, 78% respectively (Fig. 4B). For logistic regression, blood urea nitrogen (BUN) and albumin were among the lab features (Fig. 4C) predictive of mortality. The XGBoost model found most performance gain from BUN and LDH. Feature importance for predicting ventilation or ICU admission differed between models. For ventilation, logistic regression selected calcium, glucose, and CRP with large absolute coefficient values, while XGBoost identified calcium, glucose, CRP, and LDH as important features. For those admitted to ICU, XGBoost benefited from the same lab features, while monocyte percentage and carbon dioxide were additionally selected for by logistic regression. Of note, for XGBoost, no lab feature showed higher importance measure than respiration rate and SpO2 did for all three outcomes.

Finally, models trained on data collected in the last 24 hours excelled at predicting deceased. The logistic regression model (Fig. 5A) had AUC performance of 0.91, specificity of 88%, and sensitivity of 84%. The XGBoost model (Fig. 5B) had AUC performance of 0.92, specificity of 86%, and sensitivity of 85%. The importance of respiration rate increased for XGBoost (Fig. 5C), accounting for more than 50% of the gain. Values of SpO2 and age 75+ were the next most important features.

Using the same coefficients and tree weights/structures, both models were assessed based on clinical data from the preceding 30 days (Fig. 5D). With cutoffs of 0.80 for AUC, and 70% for specificity and sensitivity, logistic regression was able to predict deceased 4 days in advance (AUC = 0.82, specificity = 85%, sensitivity = 71%) and 5 days in advance (AUC = 0.81, specificity = 70%, sensitivity = 75%) for XGBoost. Models were not trained on those ventilated or ICU admitted, as these events are unlikely to occur in the final 24 hours preceding discharge/deceased. Labs were not incorporated because few blood tests were ordered in the final 24 hours.

To explore whether patient status can be dynamically predicted based on history data, we also built time series models using simple recurrent neural network (RNN), gated recurrent unit (GRU) and long short term memory (LSTM) architectures and compared the performance metrics to single time point models of logistic regression (LR) and multilayer perceptron (MLP). A major goal is to explore whether more complex modeling approaches are able to make accurate and transferrable predictions.

The vital status of each patient was converted to a time series that flagged positive for time points within 3-day intervals before the patient deceased (Fig. 6A). The time series models (RNN, GRU and LSTM) were trained to take medical data of 8 time points as input and infer the vital status at each point, giving rise to a real-time risk prediction based on historical records. The single time point models (LR and MLP), on the other hand, only use medical data at the current point to make the prediction. Model comparison was carried out with three different feature sets: vital signs (body temperature, pulse, respiration rate, systolic blood pressure, diastolic blood pressure, SpO2) only, vital signs and 46 lab results with nonzero coefficients in the single time point LASSO regression model, vital signs and lab results plus 'static' demographical information of sex, age group, diabetic history and comorbidities (Supplemental Table S3). As the time series data were recorded with uneven and irregular intervals, the progression time (in days) was included in all models as an additional feature. For models only including vital sign features, time series models showed better performance (Fig. 6B) compared to single time point models, but performance was comparable among all models when lab results and demographical information was added to the feature set.

DISCUSSION

Retrospective analysis of COVID-19 positive patients identified recognizable clinical markers such as respiration rate and SpO2, but also provided insights distinguishing morbidity (ICU admitted or ventilated outcomes) from mortality (deceased outcome). Our study confirms canonical risk factors previously established (ex. Age, respiration rate, SpO2) as predictive of mortality and morbidity, but also uncovers a surprising finding that temperature was not predictive for mortality. In addition, lab markers of physiological stress including LDH, BUN, and CRP were found to be important for model prediction, but not other canonical indicators such as procalcitonin.

Our results aligned with previous work [10] analyzing patient data from NYU Langone to predict absence of adverse events within a 96 hour window as opposed to negative outcomes. Several features of importance overlapped both studies, notably respiration rate, SpO2, LDH, BUN, and CRP. However, other selected features such as temperature, platelet count, pulse, and eosinophil percentage were not found to be important in our model.

Although the goal of stratifying patients by disease severity aligned, the different approaches likely explain the differences in variable explanation. Our study differs in that our models are trained only on clinical data from the first 24 hours after admission, as compared to continuously updating predictions when new labs are reported. Thus, features that are important for outcome prediction at time of admission will differ from those that better model variations in disease severity over time. In addition, we stratify our negative outcomes into mortality and morbidity, and separate morbidity further to compare those requiring ICU admission versus ventilation. Eosinophil percentage was statistically different between all 3 clinical outcomes, while temperature and pulse were only different for morbidity and platelet counts only for mortality (Supplemental Table S1). It is hypothesized that patients exhibiting symptoms of fever and increased pulse rate, likely a consequence of decreased SpO2 (cor = -0.21, -0.12 respectively) will likely be prioritized for ICU care and/or ventilation. Although SpO2 and respiration rate were consistently selected as predictive features across outcomes and modeling methods, age groups were informative predictors of mortality risk only. As expected, the mortality model performed better than morbidity models. These results suggest that disease severity and mortality risks may require unique modeling with different predictor subsets and weighting factors. It is also consistent with the observation that senior patients were the most vulnerable population, while mortality rate among the youth was relatively low [11].

In addition, although current evidence suggests adults with type 2 diabetes mellitus are at increased risk for COVID-19 complications, our XGBoost model did not find a past diagnosis important for predicting morbidity or mortality. Only after incorporating lab features did we identify a positive correlation between exact glucose values and poorer outcomes. Together this observation suggests that the elevated blood sugar levels observed may be the result of physiological stress triggered by the disease. Indeed, prior work has shown that even when controlled for pre-existing diabetes, hyperglycemia was commonly observed in acutely ill hospitalized patients and linked to poorer outcomes [12,13].

Other lab features also identified routine chemistry data points that shed light on disease pathology. Values of LDH were elevated for all three clinical outcomes, a finding consistent with widespread tissue damage that has been shown in numerous studies to be a predictor of morbidity and mortality in a wide variety of diseases beyond COVID-19 [14–18]. Mortality was also predicted for by BUN. To investigate further the possibility of any relations to acute kidney injury, we re-trained our models with BUN/creatinine ratio as an additional feature. While correlated with mortality (cor=0.17), the

feature was not selected for by LASSO, and was only of importance when BUN was removed from training. Indeed, recent literature has revealed that BUN is emerging as an independent predictor of mortality in a variety of diseases, including heart failure [19], aortic dissection [20], and acute pancreatitis [21]. It has also been proposed that BUN is an important indicator for metabolic diseases and general nutritional status of patients, explaining its relative importance in the prediction for mortality. The relationship here is unclear and warrants further investigation.

Interestingly, admission calcium level was a more important predictor of morbidity in our models than procalcitonin was. As a peptide precursor of calcitonin, a hormone involved in calcium homeostasis, procalcitonin is also an acute phase reactant that has been used historically (albeit controversially) to help diagnose bacterial pneumonia [22–24]. Although many studies [25–27] have described a positive relationship between procalcitonin levels and mortality and morbidity in COVID-19 patients, few have commented on the importance of calcium as a prognostic value, as we have found in our study. Calcium was negatively correlated with all 3 measured clinical outcomes, which is consistent with other studies linking hypocalcemia with increased morbidity and mortality in COVID-19 patients [28–30]. Theoretically, hypocalcemia could be a result of increased procalcitonin, since procalcitonin is the precursor of calcitonin whose function is to reduce serum calcium. Interestingly, it has been reported that in a systemic inflammatory response, serum calcitonin does not increase concordantly in response to increased procalcitonin. This situation could indicate that calcium is a predictive factor through an entirely different mechanism than the more well-established procalcitonin. One theory is that alteration of calcium homeostasis is perhaps used as a strategy by the SARS-CoV-2 virus for survival and replication since calcium is essential for virus structure formation, entry, gene expression, virion maturation and release. Another possibility is that patients who present with hypocalcemia have preexisting parathyroid hormone (PTH) and vitamin D imbalances that are exacerbated by SARS-CoV-2 infection. Our study could not evaluate the importance of PTH or vitamin D due to infrequent lab orders (0.21% and 0.08% completeness respectively).

While the inclusion of lab features resulted in only modest improvement for ventilation and ICU admission prediction, lab values did result in larger increases in performance metrics for mortality prediction. However, time series modeling failed to improve prediction performance with more clinical features. This observation is likely due to the fact that laboratory results were sampled much less frequently than vital sign readings. Moreover, treating 'static' demographical as repeating time series measurements may be suboptimal for recurrent models. As discussed above, laboratory measurements may help modeling mortality risk of patients, and future work will focus on efficiently incorporating these static features for dynamic predictions [31,32].

A key limitation of our dataset revolves around balancing inclusion criteria to maximize the number of encounters available for model training, while also limiting the amount of missing data. For example, COVID-19 positive patients presenting with less severe symptoms in outpatient or telehealth settings may not have a complete set of vital signs, or any lab values available. Similarly, past medical histories are dependent on an accurate recollection on the patient's part either through a past hospital encounter or at time of admission. In addition, it is possible that the comorbidities designation in our dataset may have false negatives. Because patient histories are often self-reported, it is possible that admitted patients with no prior encounters with the hospital, or either the physical or cognitive inability to verbalize such history at time of triage, would not have such indication available in the electronic health record. However, this reflects real-world medical situations, in which diagnoses must be made based on unverifiable patient data or delayed lab results. Finally, as data was retrospectively gathered from Epic during the early stages of the pandemic when diagnostic and treatment protocols were still being developed, a concerted effort to gather novel biomarker tests

that have later been shown to be linked with disease severity is not expected. As time draws on and new variants emerge, we also expect repeated studies will be needed to survey changes to risk factors.

DATA AVAILABILITY

The data that support the findings of this study were obtained from the Medical Center Information Technology (MCIT) at NYU Langone Health but restrictions apply to the availability of these data and so are not publicly available due to specific institutional requirements.

ACKNOWLEDGEMENTS

AUTHOR CONTRIBUTIONS

J.M. Wang, W. Liu, and D. Fenyö contributed to conception and design, data acquisition, analysis, interpretation, drafted and critically revised the manuscript.

X. Chen contributed to conception and design, analysis, interpretation, drafted and critically revised the manuscript.

M.P. McRae, and J.T. McDevitt contributed to conception and design, interpretation, and critically revised the manuscript.

FIGURE LEGENDS

Figure 1. Overview of clinical dataset. A. Patient ages were binned by predefined ranges and the ratio of outcomes compared across age groups. **B.** For each patient, hospitalization stay was normalized by length of stay and segmented into 5% windows. Within each window, all values for the measured clinical variable were averaged. Each line is colored by the 6 possible outcomes.

Figure 2. Predictive performance using clinical data from the first 24 hours. A. ROC curve and PRC for logistic regression model. **B.** ROC curve and PRC for XGBoost model. **C.** Coefficient weights for the logistic model are recorded on the left. Model performance gains for XGBoost are listed on the right.

Figure 3. Overview of lab features collected in the first 24 hours. A. t-SNE plot based on previously collected clinical features and new lab values. **B.** Pairwise Pearson correlation heatmap.

Figure 4. Predictive performance after incorporating lab features. A. ROC curve and PRC for logistic regression model. **B.** ROC curve and PRC for XGBoost model. **C.** Coefficient weights for the logistic model are recorded on the left. Model performance gains for XGBoost are listed on the right.

Figure 5. Predictive performance of deceased using clinical data from the final 24 hours. A. ROC curve and PRC for logistic regression model. **B.** ROC curve and PRC for XGBoost model. **C.** Coefficient weights for the logistic model are recorded on the left. Model performance gains for XGBoost are listed on the right. **D.** Performance of models to predict deceased outcome was assessed using clinical data from the preceding 30 days. Plots track the AUC, AUPRC, specificity, and sensitivity when using the threshold that maximized the sum of the sensitivity and specificity (Youden's J statistic).

Figure 6. Time series model performance. A. Time series labels for mortality risk. Medical measurements are obtained at time points across the admission period with uneven intervals. Green/red arrows represent time points with negative/positive (0/1) labels. **B.** Mean values of area under the precision-recall curve (AUPRC) and area under the receiver operating characteristics curve (AUROC) for five model architectures across three feature settings.

Supplemental Figure 1. Flow diagram to illustrate the number of patients at each filtering step and descriptions of the criteria that needed to be fulfilled.

Supplemental Figure 2. Effect of early ventilation treatment on vital signs. A. Distribution of averaged respiration rates for all values preceding 24 hours (top) and for all values that precede initiation of ventilation treatment (bottom). B. Distribution of averaged SpO2 for all values preceding 24 hours (top) and for all values that precede initiation of ventilation treatment (bottom).

REFERENCES

1. CDC. COVID-19 Cases, Deaths, and Trends in the US | CDC COVID Data Tracker [Internet]. Cent Dis Control Prev. 2020 [cited 2020 Nov 18]. Available from: https://covid.cdc.gov/covid-data-tracker

2. Yan L, Zhang H-T, Goncalves J, Xiao Y, Wang M, Guo Y, Sun C, Tang X, Jing L, Zhang M, Huang X, Xiao Y, Cao H, Chen Y, Ren T, Wang F, Xiao Y, Huang S, Tan X, Huang N, Jiao B, Cheng C, Zhang Y, Luo A, Mombaerts L, Jin J, Cao Z, Li S, Xu H, Yuan Y. An interpretable mortality prediction model for COVID-19 patients. Nat Mach Intell Nature Publishing Group; 2020 May;2(5):283–288. doi: 10.1038/s42256-020-0180-7

3. Yao H, Zhang N, Zhang R, Duan M, Xie T, Pan J, Peng E, Huang J, Zhang Y, Xu X, Xu H, Zhou F, Wang G. Severity Detection for the Coronavirus Disease 2019 (COVID-19) Patients Using a Machine Learning Model Based on the Blood and Urine Tests. Front Cell Dev Biol [Internet] 2020 Jul 31 [cited 2020 Oct 22];8. PMID:32850809

4. Wang D, Hu B, Hu C, Zhu F, Liu X, Zhang J, Wang B, Xiang H, Cheng Z, Xiong Y, Zhao Y, Li Y, Wang X, Peng Z. Clinical Characteristics of 138 Hospitalized Patients With 2019 Novel Coronavirus–Infected Pneumonia in Wuhan, China. JAMA 2020 Mar 17;323(11):1061. doi: 10.1001/jama.2020.1585

5. Cheng F-Y, Joshi H, Tandon P, Freeman R, Reich DL, Mazumdar M, Kohli-Seth R, Levin MA, Timsina P, Kia A. Using Machine Learning to Predict ICU Transfer in Hospitalized COVID-19 Patients. J Clin Med Multidisciplinary Digital Publishing Institute; 2020 Jun;9(6):1668. doi: 10.3390/jcm9061668

6. McRae MP, Dapkins IP, Sharif I, Anderman J, Fenyo D, Sinokrot O, Kang SK, Christodoulides NJ, Vurmaz D, Simmons GW, Alcorn TM, Daoura MJ, Gisburne S, Zar D, McDevitt JT. Managing COVID-19 With a Clinical Decision Support Tool in a Community Health Network: Algorithm Development and Validation. J Med Internet Res 2020;22(8):e22033. doi: 10.2196/22033

7. Tibshirani R. Regression Shrinkage and Selection via the Lasso. J R Stat Soc Ser B Methodol [Royal Statistical Society, Wiley]; 1996;58(1):267–288. http://www.jstor.org/stable/2346178

8. Chen T, Guestrin C. XGBoost: A Scalable Tree Boosting System. Proc 22nd ACM SIGKDD Int Conf Knowl Discov Data Min [Internet] New York, NY, USA: Association for Computing Machinery; 2016 [cited 2020 Nov 18]. p. 785–794. doi: 10.1145/2939672.2939785

9. keras-team/keras [Internet]. Keras; 2020 [cited 2020 Nov 14]. Available from: https://github.com/keras-team/keras

10. Razavian N, Major VJ, Sudarshan M, Burk-Rafel J, Stella P, Randhawa H, Bilaloglu S, Chen J, Nguy V, Wang W, Zhang H, Reinstein I, Kudlowitz D, Zenger C, Cao M, Zhang R, Dogra S, Harish KB, Bosworth B, Francois F, Horwitz LI, Ranganath R, Austrian J, Aphinyanaphongs Y. A validated, real-time prediction model for favorable outcomes in hospitalized COVID-19 patients. Npj Digit Med Nature Publishing Group; 2020 Oct 6;3(1):1–13. doi: 10.1038/s41746-020-00343-x

11. Yang W, Kandula S, Huynh M, Greene SK, Wye GV, Li W, Chan HT, McGibbon E, Yeung A, Olson D, Fine A, Shaman J. Estimating the infection-fatality risk of SARS-CoV-2 in New York City during the spring 2020 pandemic wave: a model-based analysis. Lancet Infect Dis [Internet] Elsevier; 2020 Oct 19 [cited 2020 Nov 17];0(0). PMID:33091374

12. Corathers SD, Falciglia M. The role of hyperglycemia in acute illness: Supporting evidence and its limitations. Nutrition 2011 Mar 1;27(3):276–281. doi: 10.1016/j.nut.2010.07.013

13. McCowen KC, Malhotra A, Bistrian BR. Stress-induced hyperglycemia. Crit Care Clin 2001 Jan;17(1):107–124. PMID:11219223

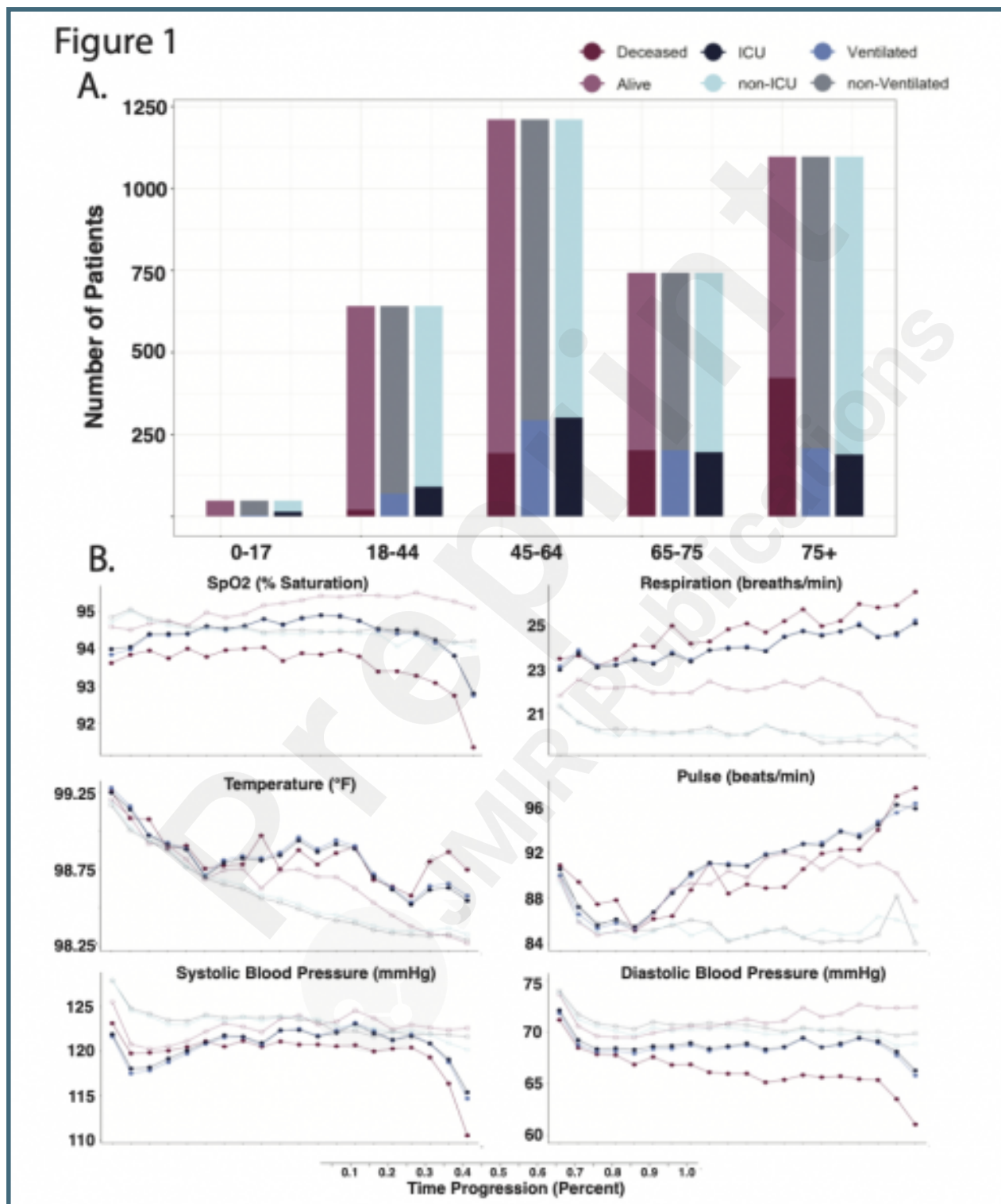14. Kishaba T, Tamaki H, Shimaoka Y, Fukuyama H, Yamashiro S. Staging of Acute Exacerbation

in Patients with Idiopathic Pulmonary Fibrosis. Lung 2014 Feb 1;192(1):141–149. doi: 10.1007/s00408-013-9530-0

15. Lam CWK, Chan MHM, Wong CK. Severe acute respiratory syndrome: clinical and laboratory manifestations. Clin Biochem Rev 2004 May;25(2):121–132. PMID:18458712

16. Chen X-Y, Huang M-Y, Xiao Z, Yang S, Chen X-Q. Lactate dehydrogenase elevations is associated with severity of COVID-19: a meta-analysis. Crit Care 2020 Jul 24;24(1):459. doi: 10.1186/s13054-020-03161-5

17. LitCovid [Internet]. [cited 2020 Nov 2]. Available from: https://www.ncbi.nlm.nih.gov/research/coronavirus/

18. Goldberg DM, Brown D. Biochemical tests in the diagnosis, classification, and management of patients with malignant lymphoma and leukemia. Clin Chim Acta 1987 Oct 30;169(1):1–76. doi: 10.1016/0009-8981(87)90394-9

19. Filippatos G, Rossi J, Lloyd-Jones DM, Stough WG, Ouyang J, Shin DD, O'Connor C, Adams KF, Orlandi C, Gheorghiade M. Prognostic Value of Blood Urea Nitrogen in Patients Hospitalized With Worsening Heart Failure: Insights From the Acute and Chronic Therapeutic Impact of a Vasopressin Antagonist in Chronic Heart Failure (ACTIV in CHF) Study. J Card Fail 2007 Jun 1;13(5):360–364. doi: 10.1016/j.cardfail.2007.02.005

20. Liu J, Sun L-L, Wang J, Ji G. Blood urea nitrogen in the prediction of in-hospital mortality of patients with acute aortic dissection. Cardiol J 2018;25(3):371–376. doi: 10.5603/CJ.a2017.0075

21. Zhou H, Mei X, He X, Lan T, Guo S. Severity stratification and prognostic prediction of patients with acute pancreatitis at early phase: A retrospective study. Medicine (Baltimore) 2019 Apr;98(16):e15275. PMID:31008971

22. Wussler D, Kozhuharov N, Tavares Oliveira M, Bossa A, Sabti Z, Nowak A, Murray K, du Fay de Lavallaz J, Badertscher P, Twerenbold R, Shrestha S, Flores D, Nestelberger T, Walter J, Boeddinghaus J, Zimmermann T, Koechlin L, von Eckardstein A, Breidthardt T, Mueller C. Clinical Utility of Procalcitonin in the Diagnosis of Pneumonia. Clin Chem 2019;65(12):1532–1542. PMID:31615771

23. Procalcitonin's Adjunct Role in the Diagnosis and Management of Pneumonia | Clinical Chemistry | Oxford Academic [Internet]. [cited 2020 Nov 2]. Available from: https://academic.oup.com/clinchem/article/65/12/1474/5715861

24. Self WH, Balk RA, Grijalva CG, Williams DJ, Zhu Y, Anderson EJ, Waterer GW, Courtney DM, Bramley AM, Trabue C, Fakhran S, Blaschke AJ, Jain S, Edwards KM, Wunderink RG. Procalcitonin as a Marker of Etiology in Adults Hospitalized With Community-Acquired Pneumonia. Clin Infect Dis Off Publ Infect Dis Soc Am 2017 Jul 15;65(2):183–190. PMID:28407054

25. Liu Z-M, Li J-P, Wang S-P, Chen D-Y, Zeng W, Chen S-C, Huang Y-H, Huang J-L, Long W, Li M, Gao R-F, Guo L, Wu X-H. Association of procalcitonin levels with the progression and prognosis of hospitalized patients with COVID-19. Int J Med Sci 2020;17(16):2468–2476. PMID:33029089

26. Hu R, Han C, Pei S, Yin M, Chen X. Procalcitonin levels in COVID-19 patients. Int J Antimicrob Agents 2020 Aug;56(2):106051. PMID:32534186

27. Liu F, Li L, Xu M, Wu J, Luo D, Zhu Y, Li B, Song X, Zhou X. Prognostic value of interleukin-6, C-reactive protein, and procalcitonin in patients with COVID-19. J Clin Virol Off Publ Pan Am Soc Clin Virol 2020;127:104370. PMID:32344321

28. Liu J, Han P, Wu J, Gong J, Tian D. Prevalence and predictive value of hypocalcemia in severe COVID-19 patients. J Infect Public Health 2020 Sep 1;13(9):1224–1228. doi: 10.1016/j.jiph.2020.05.029

29. Sun J-K, Zhang W-H, Zou L, Liu Y, Li J-J, Kan X-H, Dai L, Shi Q-K, Yuan S-T, Yu W-K, Xu H-Y, Gu W, Qi J-W. Serum calcium as a biomarker of clinical severity and prognosis in patients

with coronavirus disease 2019. Aging 2020 25;12(12):11287–11295. PMID:32589164

30. Cappellini F, Brivio R, Casati M, Cavallero A, Contro E, Brambilla P. Low levels of total and ionized calcium in blood of COVID-19 patients. Clin Chem Lab Med CCLM De Gruyter; 2020 Aug 27;58(9):e171–e173. doi: 10.1515/cclm-2020-0611

31. Miebs G, Mochol-Grzelak M, Karaszewski A, Bachorz RA. Efficient Strategies of Static Features Incorporation into the Recurrent Neural Network. Neural Process Lett 2020 Jun 1;51(3):2301–2316. doi: 10.1007/s11063-020-10195-x

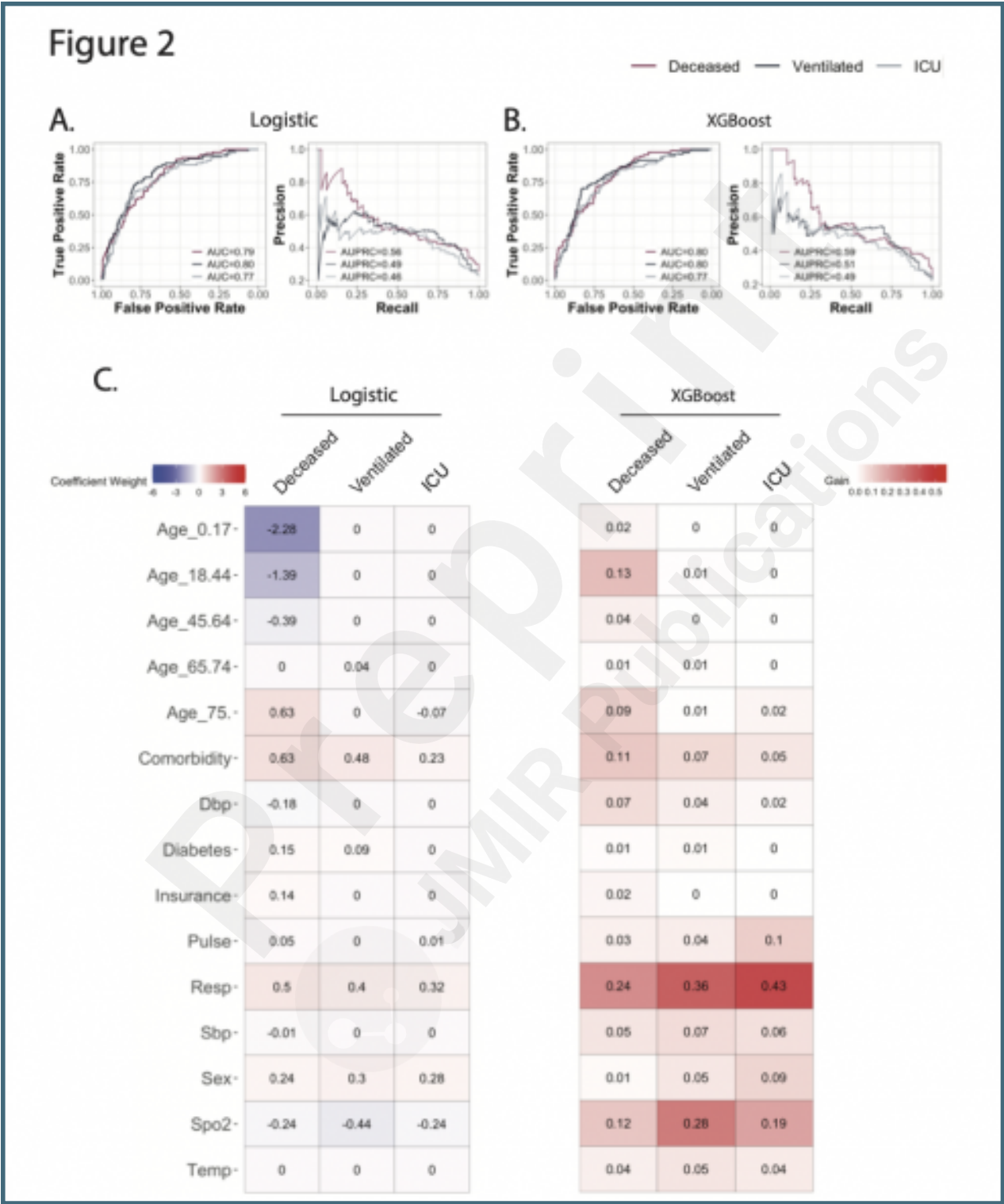32. Predicting Clinical Events by Combining Static and Dynamic Information Using Recurrent Neural Networks [Internet]. [cited 2020 Nov 14]. Available from: https://www.computer.org/csdl/proceedings-article/ichi/2016/6117a093/12OmNBBhN70

Supplementary Files

Figures

Overview of clinical dataset. A. Patient ages were binned by predefined ranges and the ratio of outcomes compared across age groups. B. For each patient, hospitalization stay was normalized by length of stay and segmented into 5% windows. Within each window, all values for the measured clinical variable were averaged. Each line is colored by the 6 possible outcomes.

Predictive performance using clinical data from the first 24 hours. A. ROC curve and PRC for logistic regression model. B. ROC curve and PRC for XGBoost model. C. Coefficient weights for the logistic model are recorded on the left. Model performance gains for XGBoost are listed on the right.

Figure 2

Overview of lab features collected in the first 24 hours. A. t-SNE plot based on previously collected clinical features and new lab values. B. Pairwise Pearson correlation heatmap.
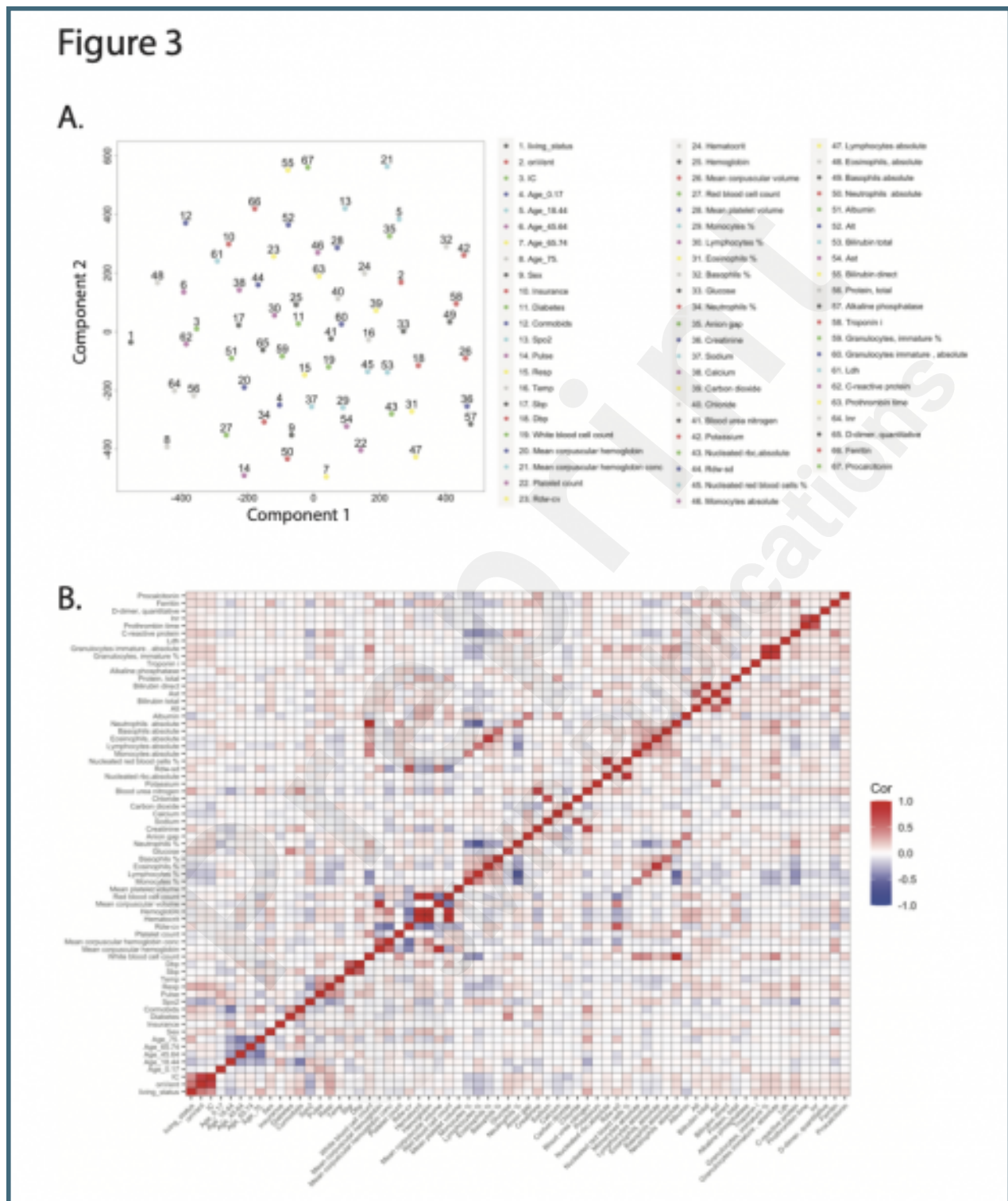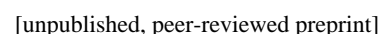
Predictive performance after incorporating lab features. A. ROC curve and PRC for logistic regression model. B. ROC curve and PRC for XGBoost model. C. Coefficient weights for the logistic model are recorded on the left. Model performance gains for XGBoost are listed on the right.
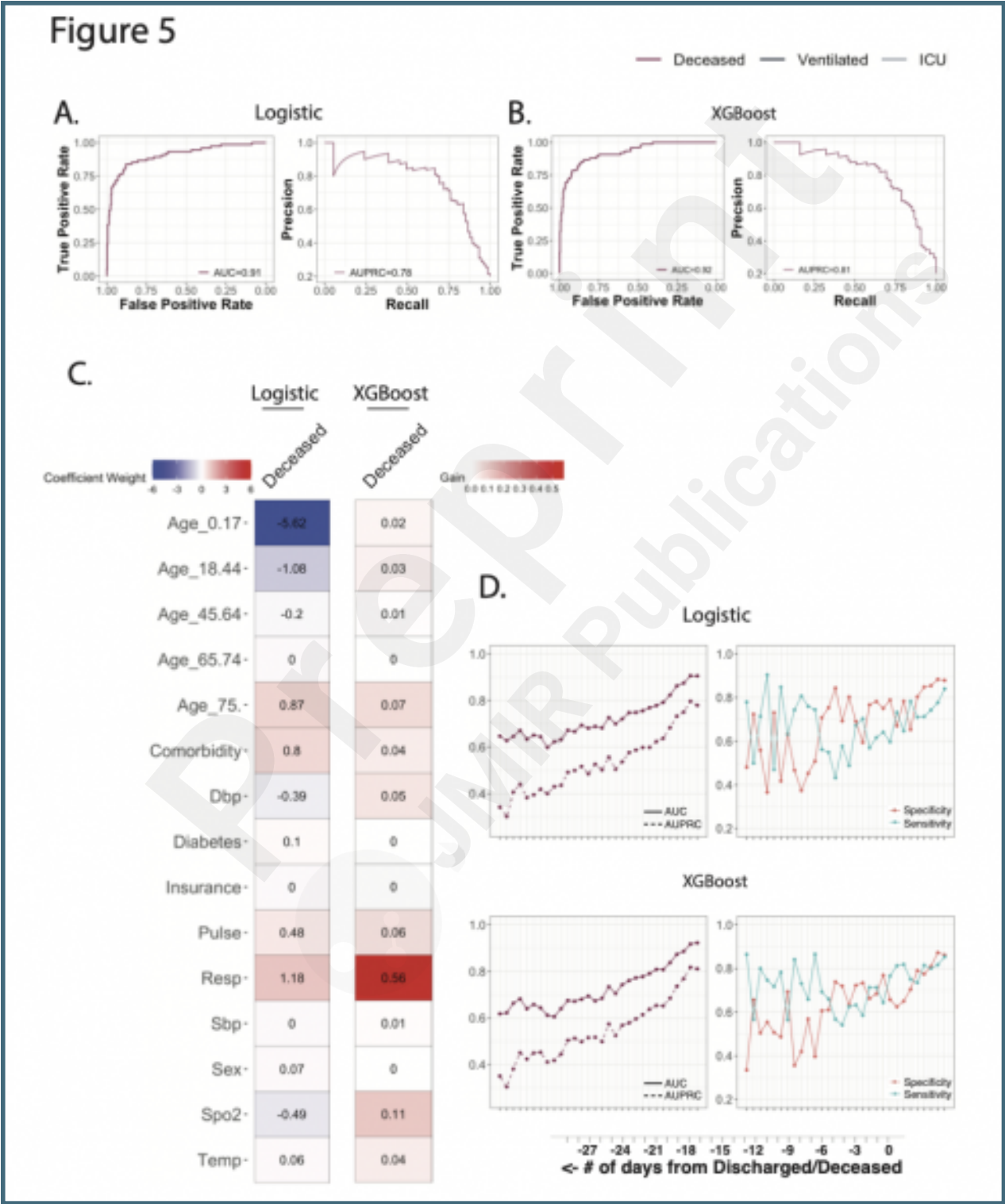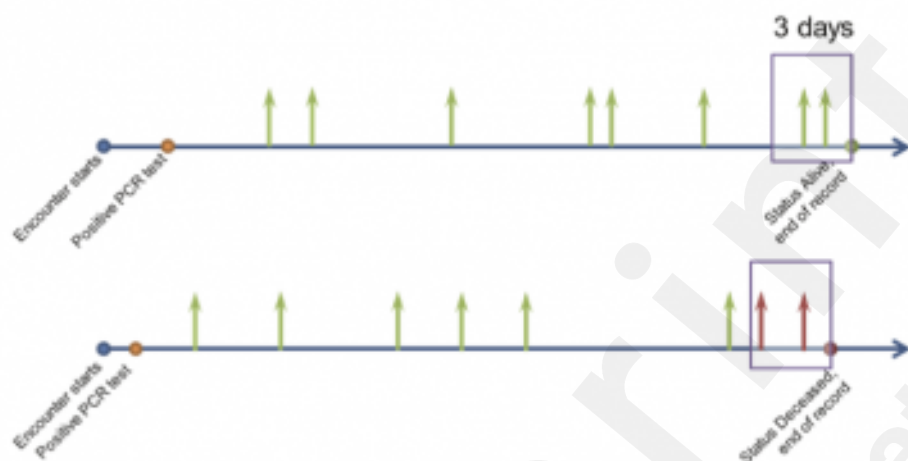

Figure 4

Predictive performance of deceased using clinical data from the final 24 hours. A. ROC curve and PRC for logistic regression model. B. ROC curve and PRC for XGBoost model. C. Coefficient weights for the logistic model are recorded on the left. Model performance gains for XGBoost are listed on the right. D. Performance of models to predict deceased outcome was assessed using clinical data from the preceding 30 days. Plots track the AUC, AUPRC, specificity, and sensitivity when using the threshold that maximized the sum of the sensitivity and specificity (Youden's J statistic).

Time series model performance. A. Time series labels for mortality risk. Medical measurements are obtained at time points across the admission period with uneven intervals. Green/red arrows represent time points with negative/positive (0/1) labels. B. Mean values of area under the precision-recall curve (AUPRC) and area under the receiver operating characteristics curve (AUROC) for five model architectures across three feature settings.
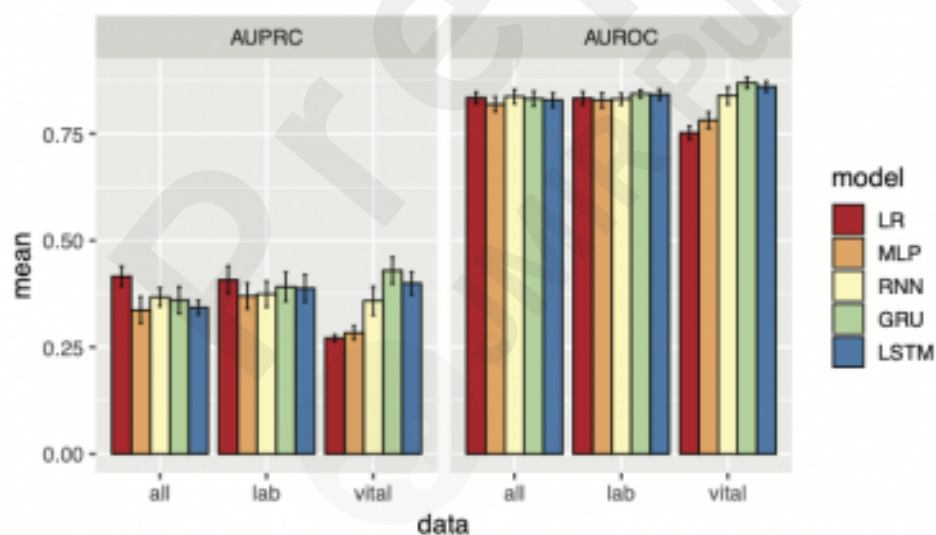
Multimedia Appendixes

Supplemental Figure 1. Flow diagram to illustrate the number of patients at each filtering step and descriptions of the criteria that needed to be fulfilled.
URL: http://asset.jmir.pub/assets/238ec8abae584ca35d0c511189e648ab.pdf

Supplemental Figure 2. Effect of early ventilation treatment on vital signs. A. Distribution of averaged respiration rates for all values preceding 24 hours (top) and for all values that precede initiation of ventilation treatment (bottom). B. Distribution of averaged SpO2 for all values preceding 24 hours (top) and for all values that precede initiation of ventilation treatment (bottom).
URL: http://asset.jmir.pub/assets/48070d94e19e64d103f4eac984303ca2.pdf

Supplemental Table S1. Demographics, vital signs, lab results, and clinical outcomes of retrospective cohort.
URL: http://asset.jmir.pub/assets/41fe00576ab9237bb4e8a5e91a6d7e45.docx

Supplemental Table S2. XGboost parameter settings for each trained model.
URL: http://asset.jmir.pub/assets/fb0d5907212f488d4ef57c7351f15ef6.docx

Supplemental Table S3. Description of features utilized for time-series modeling.
URL: http://asset.jmir.pub/assets/267cd25ed1a71029b5f3ca6cbaea75ed.docx